Electron scattering cross sections for SF_6 and SF_5CF_3 at intermediate and high energies (100–10000 eV)

P. Limão-Vieira,[1,2] F. Blanco,[3] J. C. Oller,[4] A. Muñoz,[4] J. M. Pérez,[4] M. Vinodkumar,[2,5] G. García,[6,*] and N. J. Mason[2]

[1]*Departamento de Física & Laboratório de Colisões Atómicas e Moleculares, CEFITEC, Universidade Nova de Lisboa, Quinta da Torre, 2829-516 Caparica, Portugal*

[2]*Centre of Molecular and Optical Sciences, Department of Physics and Astronomy, The Open University, Milton Keynes, MK 6AA, United Kingdom*

[3]*Departamento de Física Atómica, Molecular y Nuclear, Facultad de Ciencias Físicas, Universidad Complutense de Madrid, Avenida Complutense s/n, 28040 Madrid, Spain*

[4]*Centro de Investigaciones Energéticas Medioambientales y Tecnológicas, Avenida Complutense 22, 28040 Madrid, Spain*

[5]*V. P. & R.P.T.P. Science College, Vallabh Vidyanagr, 388 120, Gujarat, India*

[6]*Instituto de Matemáticas y Física Fundamental, Consejo Superior de Investigaciones Científicas, Serrano 113-bis, 28006 Madrid, Spain*

A modified experimental apparatus with improved angular resolution and stability has been used to measure the total electron scattering cross sections for SF_6 and SF_5CF_3 in the energy range of 100–5000 eV. A detailed analysis of the experimental error sources is provided. The experimental results are compared with integral elastic and inelastic cross sections calculated using the independent atom model approximation and a modified single-center additivity rule for electron energies ranging from 1 to 10,000 eV. The accuracy of these approximations method is discussed through a comparison with the experimental results. Previous cross-sectional data for SF_6 are compared with the present theoretical and experimental results. For SF_5CF_3, we present the first electron scattering cross-sectional data for the 100–10,000 eV energy range, as well as the first empirical determination of the molecular polarizability.

PACS number(s): 34.80.−i

I. INTRODUCTION

Total electron scattering cross sections for molecules are essential for the study of electron transport properties in gases. They define the mean-free path of electrons in the medium and, since they are the sum of all the possible collision processes, they constitute a valuable set of reference data. In the last few years, a considerable effort has been made to obtain accurate values for such cross sections due to their use in many physicochemical models of both natural and industrial processes (e.g., atmospheric auroral emissions and plasma discharges). However for intermediate and high energies, above 100 eV, accurate absolute scattering total cross sections require extremely good angular and energy resolution to avoid systematic errors arising from the detection of electrons scattered in the forward direction. Reliable experimental results are therefore scarce and a validation of data determined using different experimental techniques is necessary [1,2].

Fluorine-containing species have been extensively studied in recent years because of their use as feed gases in plasma etching reactors for silicon treatment and their role in the photochemistry of the atmosphere, mainly as ozone depleting molecules. SF_6 is of particular technical interest because of its insulating properties, being commonly used in high-voltage lines and particle accelerators. Electron scattering cross section measurements for SF_6 have been summarized by Karwasz *et al.* [3] and a set of cross-sectional data recommended for use in plasma models presented by Phelps and Brunt [4]. A complete set of electron scattering cross section values, as recommended by Christophorou and Olthoff, can be found at the NIST database web page [5]. To date, most of these measurements were obtained for electron energies below 500 eV, above this energy there are only three sets of data. Elastic cross section measurements up to 700 eV have been reported by Sakae *et al.* [6], the total electron scattering cross section data measured by Zecca *et al.* [7] in a circular Ramsauer-type apparatus [8] and total electron scattering results recently reported by Makochek-anwa *et al.* [9] over the electron energy range of 0.4–1000 eV using a linear transmission time-of-flight instrument. Theoretical studies of Dehmer *et al.* [10] and Gianturco *et al.* [11] for SF_6 have revealed the formation of shape resonances in low-energy total cross sections, below 40 eV, which were first observed by Kenerly *et al.* [12]. At higher energies, total electron scattering cross sections have been calculated by Jian *et al.* [13] using an independent atom model (IAM) [14] and more recently a similar technique has been applied by Joshipura *et al.* [15] providing results for both the ionization and excitation cross sections.

SF_5CF_3 has only recently been detected in the terrestrial atmosphere [16] and was swiftly identified as a potent greenhouse gas with an annual growth rate of 6%. It has the highest radiative forcing on a per molecule basis of any atmospheric pollutant [16,17]. However, its origins are still unclear but it is believed to be purely anthropogenic in origin, probably being related to the plasma technology industry and gas dielectrics being linked to the SF_6 cycle, a relation-

───────

*Corresponding author: G.Garcia, Instituto de Matematicas y Fisica Fundamental, Consejo Superior de Investigaciones Cientificas, Serrano 113-bis, 28006 Madrid, Spain. Email address: g.garcia@imaff.cfmac.csic.es

ship which is sustained by its annual growth rate tending to very closely follow that of SF_6.

The spectroscopy, dissociation dynamics, and chemical reactivity of SF_5CF_3 are still poorly understood having only been the subject of research in the last two years (see e.g., Ref. [18–25]). There has been much speculation as to the mechanisms by which SF_5CF_3 is destroyed in the terrestrial atmosphere with current suggestions including: (i) UV photodissociation in the stratosphere and mesosphere [17–20], (ii) electron attachment and ion-molecule reactions in the mesosphere [21–24], and (iii) by reactions on ice or dust surfaces [25]. Kennedy and Mayhew [26] have made a comprehensive study of the electron attachment rate constant and comparisons with their data at low energy were made by Märk and co-workers [21] using a high-resolution electron-beam and anion mass spectrometry. Märk and co-workers also reported electron impact ionization cross sections close to threshold [27] and discussed the role of SF_5CF_3 in the terrestrial atmosphere. Recently, a high-resolution VUV photoabsorption spectrum of SF_5CF_3 has been measured using synchrotron radiation in the range from 5.5 eV to 10.8 eV and compared with an electron energy loss spectrum in pseudo-optical conditions such that the electronic state spectroscopy of SF_5CF_3 may be evaluated [20].

In this paper, we present total electron scattering cross section measurements from 100 to 5000 eV incident energies both for SF_6 and SF_5CF_3. The experimental apparatus is based on an earlier design used in previous studies [1,2], but has been modified in order to improve the angular resolution and the electron current stability, therefore reducing the experimental uncertainties to lower than 3%. Results for SF_6 are compared with previous measurements available in the literature, while for SF_5CF_3 we believe that these are the first measurements to be reported.

Integral elastic and inelastic cross sections for electron energies ranging from 1 to 10 000 eV have been calculated for these molecules through an optical potential method in the framework of the independent atom approximation [14]. Screening corrections have been introduced into the calculation to take into account the partial overlapping of atoms in the molecule. The reliability and limitation of this approximate method is discussed by comparison with experimental results.

These calculations are in turn compared with the results of a modified single center additivity rule (MSCAR) which incorporate the molecular structure through a semiempirical procedure [15]. More details on these two methods are given below.

Finally, the suitability of the empirical formula derived previously [28] for the high-energy electron scattering cross sections for some molecular targets is discussed for these molecules. As a consequence of this analysis, an empirical value for the molecular polarizability of SF_5CF_3 is deduced.

II. EXPERIMENT

A. Experimental apparatus and procedure

Absolute electron scattering cross sections have been measured in a transmission beam system for incident ener-
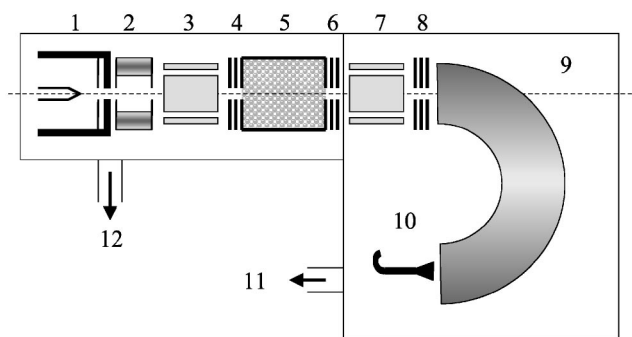

FIG. 1. Experimental apparatus: (1) Electron gun, (2) transverse magnetic field, (3, 7) quadrupole electrostatic plates, (4, 6, 8) decelerating and accelerating lenses, (5) scattering chamber, (9) hemispherical electrostatic energy analyzer, (10) channel electron multiplier, and (11, 12) vacuum turbopumps.

gies between 100 and 5000 eV. The experimental apparatus is based on a system described in previous papers [1,2], but important modifications have been introduced in order to improve the angular resolution and the electron current stability and to reduce the lower-energy limit to 100 eV. A schematic diagram of the apparatus is shown in Fig. 1. The primary beam is produced from a negatively biased electron filament. A combination of transverse magnetic fields and an electrostatic plate system control both the beam direction and reduce the energy spread to 100 meV. The electron beam is then collimated by a 0.7 mm diameter diaphragm placed 5 mm in front of the entrance aperture of the interaction region. This electrode is grounded through a current integrator that controls the total current emitted by the filament during the measurements. The collision chamber is formed by two apertures of 1 and 2 mm diameter, respectively, separated by 50 mm. This length can be extended to 100 mm when required. With this geometry, the beam diameter is smaller than the apertures of the gas cell, avoiding undesired plasma focusing effects in the surrounding area of the chamber apertures. Typical electron currents in the chamber were of the order of 10^{-13} A. The entire collision chamber was placed at a negative potential. The electron kinetic energy in the interaction chamber is then defined by the difference between the potential applied to the cathode and the potential applied to the chamber where attenuation takes place. This method allows us to lower the energy of the electron beam to 100 eV without requiring any additional shielding against stray electric and magnetic fields.

The gas pressure in the chamber was measured using an absolute capacitance nanometer (MKS Baratron 127A) and two Pirani gauges, previously calibrated for both SF_6 and SF_5CF_3. At the exit of the collision chamber, an electrostatic quadrupole plate system selects the direction of the transmitted electrons. The transmitted electrons are energy analyzed by a hemispherical electrostatic spectrometer and finally detected by a channel electron multiplier detector working in single-pulse counting mode. The energy resolution of the analyzer was 0.5% with respect to the transmission energy. By retarding the electron beam at the entrance of the analyzer with a three-element lens, a constant resolution of 0.5 eV has been achieved over the whole energy range con-
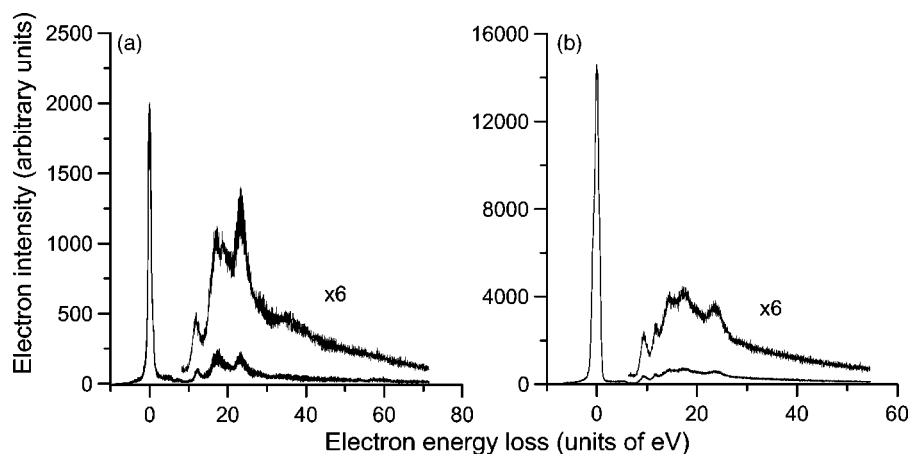
FIG. 2. Electron energy loss spectra for 2000 eV electrons interacting with 20 mTorr of (a) SF$_6$ and (b) SF$_5$CF$_3$, respectively.

sidered here. The maximum angular acceptance of the energy analyzer was 1.9×10^{-5} sr. The system was differentially pumped by two turbopumps of 70 and 250 l/s, respectively, reaching a background pressure of 10^{-8} Torr. The pressure in the electron gun and analyzer region was maintained lower than 10^{-6} Torr during the measurements.

B. Error analysis

The main sources of error in this experiment have been discussed in detail elsewhere [1,2], so only the modifications introduced into the experiment will be discussed here. The current integrator provides an automatic normalization procedure with respect to variations in the primary beam current. A total amount of charge is set in the integrator and the storage time of each measurement adjusted to reach this charge value. Under these conditions, statistical uncertainties were of the order of 1%. However, the new scattering chamber, which allows a negative potential polarization to reduce the impact energy, requires some insulators in the gas entrance and pressure gauge connections, introducing a variation in the pressure along the gas cell of about 2%.

Systematic errors in the new scattering geometry have been evaluated by measuring the total electron scattering cross sections for N$_2$ from 1000 to 5000 eV and comparing the results with our previous measurements [29]. A general agreement (within 3%) between both experimental results was found.

It is well known [30,31] that the main systematic errors are those arising from an improper discrimination against electrons scattered into the acceptance angle of the detector, i.e., those originating from poor angular and energy resolution. The energy resolution used in this experiment was sufficient to discriminate the inelastically scattered electrons from elastically scattered electrons in the forward direction. An energy spectrum of 2000 eV electrons transmitted through 20 mTorr of SF$_6$ in the gas cell is shown in Fig. 2. This figure shows the excellent discrimination against the inelastic component of the transmitted intensity. As we have previously shown [30], an accurate way to evaluate the contribution of the elastic component is to perform Monte Carlo simulations of the electron transport through the gas cell using, as input parameters, the corresponding differential and

integral electron scattering cross sections. For this purpose, we make use of a simulation program recently developed by us [32,33]. This procedure allows us to evaluate the relative error introduced in the total cross section measurements by electrons scattered into the acceptance angle of the detector. The results of these errors are plotted in Fig. 3, the error is found to increase roughly exponentially with energy, giving a maximum contribution of about 3% at 5000 eV.

A quadratic combination of all the error sources considered here gives a total uncertainty for the measured total cross sections of less than 3%, in excellent agreement with the test measurements carried out using nitrogen as the calibrant gas.

III. CALCULATIONS

Adapting the optical potential model calculation we developed for electron scattering from atoms and extending it to molecules through an independent atom representation, the differential and integral elastic electron scattering cross
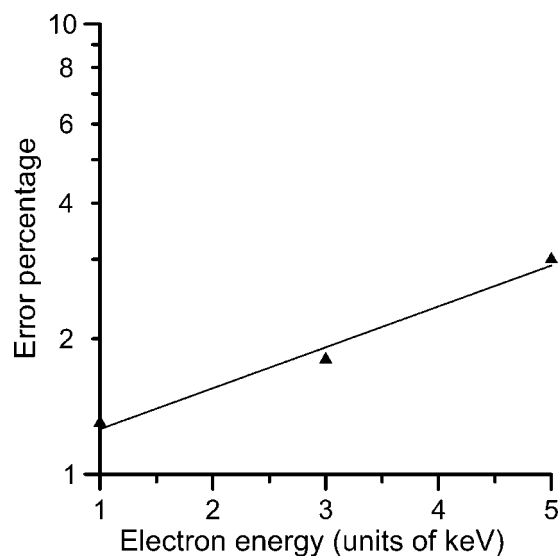

FIG. 3. Error contribution to the total cross section measurement, in percentages, of the elastically scattered electrons into the acceptance angle of the detector.
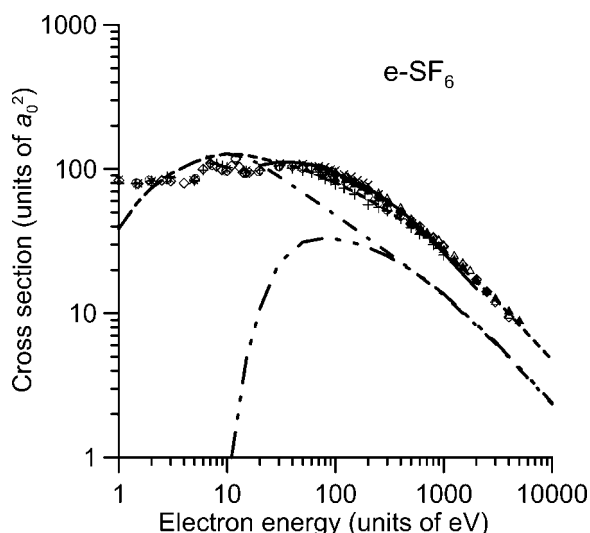
FIG. 4. Integral electron scattering cross sections for SF_6. Experimental total electron scattering cross section data: ▲, Present study; △, from Ref [7]; ○, from Ref [40]; ×, from Ref. [39]; +, from Ref. [9]; ◇, recommended values from NIST [5]. Present IAM calculations: – –, total electron scattering cross sections; —·—, integral elastic cross sections; —··—, integral inelastic cross sections. Present MSCAR calculations: —, total electron scattering cross sections.

FIG. 5. Integral electron scattering cross sections for SF_5CF_3. ▲, Experimental total electron scattering cross section data. Present calculations IAM calculations: – –, total electron scattering cross sections; —·—, integral elastic cross sections; —··—, integral inelastic cross section. Present MSCAR calculations: —, total electron scattering cross sections.

sections as well as the integral inelastic have been calculated (IAM). This calculation includes all successive improvements we have introduced in different parts of the potential: A nonempirical absorption potential for inelastic scattering [34], a local velocity correction during the collision [35], relativistic and many-body effects [36], and finally a correction procedure involving screening which significantly improves results at low energy both for integral [37] and differential [38] cross sections. Integral elastic and inelastic, as well as total electron scattering cross sections for SF_6 and SF_5CF_3 obtained by this calculation procedure, are plotted in Figs. 4 and 5, respectively, and listed in Table I.

In the second model a MSCAR is used to calculate the total scattering cross section. The method is based upon the use of a complex scattering potential, generated from the spherically averaged charge densities of the target molecule. The molecule is reduced to single center and the molecular properties of the target, such as ionization energy, bond length, and polarizability, are used as the basic input parameters [15]. The mode is further modified by incorporating the screening of the inner electrons by the outer ones, and consequently correcting the absorption potential [36].

IV. RESULTS

Both experimental and calculated total electron scattering cross sections for SF_6 and SF_5CF_3 are plotted in Figs. 4 and 5, respectively. A detailed analysis of Fig. 4 for SF_6 shows that, for energies above 100 eV, the experimental data are in excellent agreement with the earlier results reported by Zecca *et al.* [3], Karsperski [39], Dababneh [40], Sueoka [9], and those values recommended by Christophorou *et al.* [5].
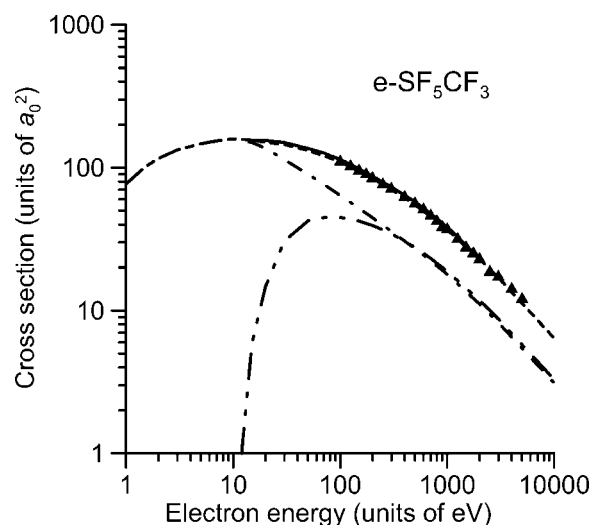
The experimental data may also be compared with the results of our approximate calculations labelled as IAM and MSCAR. Both calculations assume that, if the electron energy is high enough, the IAM is valid [14], hence the two calculations are in excellent agreement with the experiments at higher energies. For energies below 100 eV, our IAM calculation tends to overestimate the experimental cross section data reaching discrepancies of the order of 20% around 20 eV. Lower than this limit, our calculated data should be considered as a rough estimation. However, the MSCAR model fit the experimental results well even at 20 eV.

In the case of SF_5CF_3, there are no other experimental data with which to compare the present results and hence validate our cross-sectional values deviations. However, we have performed simple scattering calculations and observed that both IAM and MSCAR models predict the same cross-sectional value which are in excellent agreement with experiment.

The molecular polarizability of SF_5CF_3 can be derived from the molecular polarizability of SF_6 and their respective number of electrons and total electron scattering cross sections, according to the following equation [28]:

$$\frac{\alpha'}{a_0^3} = \frac{\alpha}{a_0^3} + \frac{10}{E(\text{keV})^{-0.78}}\left(\frac{\sigma_T'}{a_0^2} - \frac{\sigma_T}{a_0^2}\right) + 4(Z' - Z), \quad (1)$$

where α' and α are the respective polarizabilities, σ_T' and σ_T are the corresponding total cross sections for an incident energy E, in keV, and Z, Z' are the respective number of electrons in the molecular target. Applying Eq. (1) for energies ranging from 1 to 5 keV, an average value of 55 ± 7 atomic units (a_0^3) has been obtained for the molecular polarizability of SF_5CF_3.

TABLE I. Experimental and theoretical total electron scattering cross sections from SF$_6$ and SF$_5$CF$_3$ (in units of a_0^2).

Electron energy (eV)	SF$_6$			SF$_5$CF$_3$		
	Experiment	Calculations		Experiment	Calculations	
		IAM	MSC		IAM	MSC
1		38.6			76.9	
1.5		59.2			101	
2		74.0			116	
3		92.8			133	
5		112			147	
7		122			154	
10		128			159	
15		125			156	155
20		119	106		151	155
30		111	112		145	150
40			112			142
50		99.8	110		132	136
60			107			131
70			104			127
75		88.8			119	
80			101			122
90			97.5			118
100	85.2	80.7	94.0	110.0	109	114
125	84.0		87.1	102.0		105
150	77.6	69.4	81.4	95.0	94.1	98.2
175	73.9		76.4	89.4		91.9
200	69.6	61.7	73.5	84.3	84.0	87.2
250	62.3		66.1	76.1		79.1
300	57.4	51.6	60.3	71.0	70.4	73.3
400	49.8		51.6	62.1		64.0
500	42.0	40.1	44.7	55.9	54.8	57.7
600	37.1		39.3	50.8		52.0
700	34.6	33.3	35.1	46.0	45.5	47.6
800	31.9		31.6	42.1		44.2
900	29.2		28.7	38.3		40.9
1000	27.4	26.9	26.2	36.8	36.7	38.3
1250	23.3		21.7	31.6		32.8
1500	20.8		18.7	27.5		28.5
1750			16.5	25.1		25.3
2000	16.6	16.9	14.8	22.8	23.0	22.8
2500	14.2			18.6		
3000	12.6	12.5		17.2	17.0	
4000	10.3	10.0		14.1	13.6	
5000	8.82	8.40		12.0	11.3	
10 000		4.75			6.38	

V. CONCLUSIONS

Total electron scattering cross sections for SF_6 were measured in the energy range of 100–10,000 eV and are in good agreement with previous experimental data. We present the first measurements of the total cross section for electron scattering by SF_5CF_3 in the energy range of 100–10,000 eV. The experimental data are compared with calculations obtained by two different procedures, using an optical potential in the IAM approximation and a MSCAR, respectively. It is shown that "screening terms" are needed in order to account for the partial overlapping of atoms in the molecule. Once corrected for such effects, the calculated data are found to be compatible with experiment over the entire energy range from 10 to 1000 eV. This gives us confidence that such a treatment may be used to predict cross sections from species that we cannot measure in the laboratory [e.g., free radical species CF_x ($x=1$ to 3) important in silicon etching plasmas] and biological targets.

[1] G. García and F. Manero, Phys. Rev. A **57**, 1069 (1998).

[2] F. Manero, F. Blanco, and G. García, Phys. Rev. A **66**, 032713 (2002).

[3] G. P. Karwasz, R. S. Brusa, and A. Zecca, Riv. Nuovo Cimento **24**, 93 (2001), and references therein.

[4] A. V. Phelps and R. J. Van Brunt, J. Appl. Phys. **64**, 4269 (1988).

[5] L. G. Christophorou and J. K. Olthoff, Electron Interactions with SF_6, NIST Ref. Data Ser., http://www.eeel.nist.gov/811/refdata/sf6/cross.htm.

[6] T. Sakae, S. Sumiyoshi, E. Murakami, Y. Matsumoto, K. Ishibashi, and A. Katase, J. Phys. B **22**, 1385 (1989).

[7] A. Zecca, G. Karwasz, and R. S. Brusa, Chem. Phys. Lett. **199**, 423 (1992).

[8] G. Dalba, P. Fornasini, R. Grisenti, R. Lazzizzera, J. Ranieri, and A. Zecca, Rev. Sci. Instrum. **52**, 979 (1981).

[9] C. Makochekanwa, M. Kimura, and O. Sueoka, Phys. Rev. A **70**, 022702 (2004).

[10] J. Dehmer, J. Siegel, and D. Dill, J. Chem. Phys. **69**, 5205 (1978).

[11] F. A. Gianturco, R. R. Lucchese, and N. Sanna, J. Chem. Phys. **102**, 5743 (1995).

[12] R. E. Kennerly, R. A. Bonham, and M. McMillan, J. Chem. Phys. **70**, 2039 (1979).

[13] Y. Jian, J. Sun, and L. Wan, Phys. Rev. A **52**, 398 (1995).

[14] N. F. Mott and H. S. W. Massey, *The Theory of Atomic Collisions*, 3rd ed. (Clarendon, Oxford, 1971).

[15] K. N. Joshipura, M. Vinodkumar, C. G. Limbachiya, and B. K. Anthony, Phys. Rev. A **69**, 022705 (2004).

[16] P. A. Kendall, N. J. Mason, G. A. Buchanan, G. Marston, P. Tegeder, A. Dawes, S. Eden, P. Limão-Vieira, and D. A. Newnham, Chem. Phys. **287**, 137 (2003).

[17] W. T. Sturges, T. J. Wallington, M. D. Hurley, K. P. Shine, K. Shira, A. Engel, D. E. Oram, S. A. Penkett, R. Mulvaney, and C. A. M. Brenninkmeijer, Science **289**, 611 (2000).

[18] R. Y. L. Chim, R. A. Kennedy, and R. P. Tuckett, Chem. Phys. Lett. **367**, 697 (2003).

[19] P. Limão-Vieira, P. A. Kendall, S. Eden, N. J. Mason, J. Heinesch, M.-J. Hubin-Franskin, J. Delwiche, and A. Giuliani, Radiat. Phys. Chem. **68**, 193 (2003).

[20] P. Limão-Vieira, S. Eden, P. A. Kendall, N. J. Mason, A. Giuliani, J. Heinesch, M.-J. Hubin-Fraskin, J. Delwiche, and S. V. Hoffmann, Int. J. Mass. Spectrom. **233**, 335 (2004).

[21] W. Sailer, H. Drexel, A. Pelc, V. Grill, N. J. Mason, E. Illenberger, J. D. Skalny, T. Mikoviny, P. Scheier, and T. D. Märk, Chem. Phys. Lett. **351**, 71 (2002).

[22] C. Atterbury, R. A. Kennedy, C. A. Mayhew, and R. P. Tuckett, Phys. Chem. Chem. Phys. **3**, 1949 (2001).

[23] C. Atterbury, A. D. J. Critchley, R. A. Kennedy, C. A. Mayhew, and R. P. Tuckett, Phys. Chem. Chem. Phys. **4**, 2206 (2002).

[24] S. T. Arnold, T. M. Miller, A. A. Viggiano, and C. A. Mayhew, Int. J. Mass. Spectrom. **223**, 403 (2003).

[25] R. Balog, M. Stano, P. Limão-Vieira, C. König, I. Bald, N. J. Mason, and E. Illemberger, J. Chem. Phys. **119**, 10396 (2003).

[26] R. A. Kennedy and C. A. Mayhew, Int. J. Mass. Spectrom. **206**, i (2001).

[27] B. Gstir, G. Hanel, J. Fedor, M. Probst, P. Scheier, N. J. Mason, and T. D. Märk, J. Phys. B **35**, 2567 (2002).

[28] G. García and F. Manero, Chem. Phys. Lett. **280**, 419 (1997).

[29] G. García, M. Roteta, and F. Manero, Chem. Phys. Lett. **264**, 589 (1997).

[30] G. García, M. Roteta, and F. Manero, Chem. Phys. Lett. **264**, 589 (1997).

[31] G. García, J. L. de Pablos, F. Blanco, and A. Williart, J. Phys. B **35**, 4657 (2002).

[32] A. Roldán, J. M. Pérez, A. Williart, F. Blanco, and G. García, J. Appl. Phys. **95**, 5865 (2004).

[33] A. Muñoz, J. M. Pérez, G. García, and F. Blanco, Nucl. Instrum. Methods Phys. Res. A **536**, 176 (2004).

[34] F. Blanco and G. García, Phys. Lett. A **255**, 147 (1999).

[35] F. Blanco and G. García, Phys. Lett. A **295**, 178 (2002).

[36] F. Blanco and G. García, Phys. Rev. A **67**, 022701 (2003).

[37] F. Blanco and G. García, Phys. Lett. A **317**, 458 (2003).

[38] F. Blanco and G. García, Phys. Lett. A **330**, 230 (2004).

[39] G. Kasperski, P. Mozejko, and C. Szmytkowski, Z. Phys. D: At., Mol. Clusters **42**, 187 (1997).

[40] M. S. Dababneh, Y.-F. Hsieh, W. E. Kauppila, C. K. Kwan, S. J. Smith, T. S. Stein, and M. N. Uddin, Phys. Rev. A **38**, 1207 (1988).